Copy 5
RM E52K24

NACA RM E52K24

RESEARCH MEMORANDUM

ALTITUDE PERFORMANCE OF A 20-INCH-DIAMETER RAM-JET ENGINE INVESTIGATED IN A FREE-JET FACILITY AT MACH NUMBER 3.0

By George R. Smolak and Carl B. Wentworth

Lewis Flight Propulsion Laboratory
Cleveland, Ohio

NATIONAL ADVISORY COMMITTEE
FOR AERONAUTICS

WASHINGTON

June 15, 1953

NACA RM E52K24

RESEARCH MEMORANDUM

ALTITUDE PERFORMANCE OF A 20-INCH-DIAMETER RAM-JET ENGINE INVESTIGATED IN A FREE-JET FACILITY AT MACH NUMBER 3.0

By George R. Smolak and Carl B. Wentworth

SUMMARY

The performance of a 20-inch-diameter ram-jet engine was investigated at Mach number 3.0 (inlet total temperature, 1100° R) in a free-jet facility at the Lewis laboratory over a range of simulated altitudes from 60,500 to 66,500 feet.

The maximum combustor efficiency, about 0.90, occurred at fuel-air ratios between 0.04 and 0.05 over the entire range of simulated altitudes investigated. The range of exhaust-nozzle total pressures was from 1240 to 2592 pounds per square foot absolute. Lean blow-out was encountered for operation at fuel-air ratios leaner than approximately 0.029. At a 63,800-foot altitude and 0.07 fuel-air ratio, the diffuser total-pressure recovery was 0.55 and the internal thrust coefficient was 0.73. The critical value of the diffuser total-pressure recovery was 0.66.

INTRODUCTION

An investigation was conducted to determine the altitude performance characteristics of the 20-inch-diameter XRJ-43-MA1 ram-jet engine in a free-jet facility at Mach number 3.0 at the NACA Lewis laboratory. This engine was designed to power an altitude-launched research vehicle. Flight plan specifications indicate that the vehicle will be launched at an altitude of approximately 30,000 feet and rocket-boosted to a Mach number of 2.1. Upon separation of the rocket booster, the engine will provide the vehicle with sufficient thrust to enable it to climb to cruise altitudes and accelerate to the cruise Mach number of 3.0. As the vehicle cruises at Mach number 3.0, it will gradually climb to a maximum altitude of 80,000 feet.

The free-jet facility (ref. 1) and engine characteristics permitted investigation of the engine over a range of altitudes from 60,500 to 66,500 feet at a flight Mach number of 3.0 (inlet total temperature, 1100° R). The range of fuel-air ratios investigated was from lean blow-out to an arbitrary limit of 0.075. For the range of altitudes reported

herein, the vehicle flight plan requires that the engine be capable of operating over a range of fuel-air ratios from 0.035 to 0.065 with combustor efficiencies of about 0.9. Because of compromises required in the design of a fixed-geometry engine, this ram-jet engine was incapable of critical operation at a Mach number of 3.0. Consequently, this investigation was only for supercritical operation. Close simulation of ram-jet inlet conditions was provided in the free-jet facility. The cowl of the engine was enclosed in the jet and air was spilled around the inlet in the same manner as would occur in flight.

In order that the engine performance characteristics could be well defined, the following variables have been included in this report: engine air flow, diffuser Mach number profiles, combustor efficiency, combustor pressure ratio, combustor pressure, combustion-chamber-inlet Mach number, and internal thrust coefficient.

APPARATUS

Engine

Over-all dimensions. - The important details of the engine construction are shown in figure 1. The length of the engine from the tip of the dummy probe to the minimum area of the exhaust nozzle was 144 inches. The subsonic-diffuser exit, which was in the plane of the open ends of the flame-holder gutters, was 76.62 inches from the geometrical tip of the 20.5° half-angle cone. The first 8 inches of the cowl was constructed in the same manner as the flight cowl; the remainder of the engine construction was of the "boiler-plate" type. The combustion chamber was 48 inches long and was followed by a converging exhaust nozzle which had a minimum area of 55 percent of the combustion-chamber area. The flight nozzle would have a divergent section (1.69 expansion ratio) attached to the nozzle.

Diffuser. - The two-shock diffuser (fig. 1) was constructed of a 20.5° half-angle cone followed by a 15° turn formed by a 35.5° half-angle cone. A dummy total-pressure probe 3/8 inch in diameter extended 4.47 inches ahead of the geometrical tip of the 20.5° cone. The diameter of the cowl lip was 15.40 inches, and its inner contour made an angle of 27.25° with the center line of the engine. The lip of the cowl was located 18.23 inches downstream of the geometrical tip of the 20.5° cone. An annular passage formed by the outer shell and the inner body followed the supersonic-diffuser cones. There was no internal contraction in the annular passage. The maximum diameter of the inner body was just downstream of the cowl lip. Downstream of this maximum diameter the inner body was conically shaped (cone half-angle was 4.15°). The last few inches of the inner body curved at a slightly greater slope inward to a blunt end. The annular subsonic-diffuser passage was divided into

three channels by inner body support struts which extended the entire length of the subsonic diffuser.

Flame holder. - The flame holder (fig. 2) and pilot can were built integrally with the pilot can mounted on the blunt end of the inner body. The pilot can was 6 inches in diameter and 8 inches long. Louvers near the upstream end of the pilot can provided air for pilot combustion. Three gutters, which were 3 inches wide at the open end, radiated from the downstream end of the pilot can. The gutters formed channels 4.44 inches deep and were mounted on the blunt ends of the inner body support struts. Two 1-inch-wide circular 60° V-gutters at radii of 6.00 and 8.50 inches interconnected the radial gutters. Total blockage of the flame holder was 55 percent of the combustion-chamber area.

Fuel system. - The fuel injection system consisted of 27 variable-area fuel nozzles (fig. 3) spraying in a downstream direction and located 17 inches upstream of the plane of the flame holder. The nozzles were located in two concentric circular manifolds, each of which was composed of three segments (fig. 3). This segmented construction was necessitated by the presence of the inner body support struts. Each outer manifold segment was equipped with five equally spaced fuel nozzles, and each inner manifold segment had four equally spaced fuel nozzles. A single fixed-area fuel nozzle supplied fuel to the pilot can. Pilot ignition was accomplished by use of a propane igniter which extended radially into the pilot can. The fuel used for the pilot nozzle and main manifolds was MIL-F-5624 grade JP-3.

Facility

The engine was installed at zero angle of attack in the free-jet facility as shown in figure 4. Details of the construction of the facility are given in reference 1. For convenience, the essential features of the facility are repeated. A turbojet combustor section was used as a preheating mechanism for the air passing through the facility. The surge chamber, which supplied air to the free-jet nozzle, was equipped with screens and a baffle to give smooth flow to the supersonic nozzle. The supersonic nozzle had an exit Mach number of 3.0 and an exit diameter of 24.55 inches. A correction for the presence of boundary layer was included in the supersonic-nozzle contour. The Mach cone from the supersonic-nozzle lip extended just downstream of the cowl lip; therefore, the flow entering the engine was not influenced by jet chamber pressures. The inner cone of a variable-area jet diffuser intercepted the exterior surface of the cowl several inches downstream of the cowl lip. The function of the variable-area jet diffuser was to recover part of the total pressure of the flow passing around the engine, and thus permit operation with existing compressors and exhausters. Water-spray cooling and a throttling valve were provided

in the cooler section into which the engine exhaust nozzle discharged. The valve was useful in throttling the combustion chamber for starting the engine, and in investigating nonburning performance of the subsonic diffuser.

Instrumentation

Engine instrumentation (fig. 1) included (1) a 7-point static-pressure survey on the diffuser cone, (2) a 3-point static- and total-pressure survey across the inlet annulus at station 1, (3) a 16-point total-pressure and 14-point static-pressure survey at station 2, and (4) a 6-point total-pressure survey at the exhaust-nozzle inlet (station 4). Fuel flows were measured with rotameters.

Facility instrumentation (fig. 4) included total-pressure and total-temperature surveys within the surge tank. In addition, a shadowgraph was installed in the jet chamber of the facility (see fig. 4) to provide a means for observing shock patterns at the engine inlet. As shown in figure 1, the field of view of the image included the inlet annulus, the 15° turn formed by the intersection of the two upstream supersonic-diffuser cones, and the supercritical oblique shock pattern.

PROCEDURE

Supersonic flow was established by setting the jet-diffuser area to a favorable value, opening the air supply and exhaust valves, and adjusting the combustion preheater to maintain the inlet total temperature at 1100° R to simulate the standard temperature at a Mach number of 3.0 for the altitude range covered. The inlet total pressure was adjusted to simulate the desired altitude.

The engine exhaust nozzle was throttled by the valve in the spray-cooler section in order to determine the critical diffuser total-pressure recovery ratio and to provide favorable combustion-chamber-inlet conditions for igniting the burner (a pressure of about 2100 lb/sq ft abs and a velocity of about 230 ft/sec).

Shortly after the igniter was lighted, fuel was supplied to the pilot-can nozzle. Upon ignition of the pilot fuel, the propane igniter was turned off and fuel was supplied to the two fuel injection manifolds. As flame seated on the two circular flame-holder gutters, the pressure in the combustion chamber increased rapidly, tending to expel the normal shock from the diffuser; consequently, it was necessary simultaneously to open the spray-cooler throttling valve to reduce this pressure. With the 55-percent exhaust nozzle it was theoretically impossible to reach critical recovery at any fuel-air ratio for operation at a Mach number of 3.0.

[redacted]

The pilot was used for all burning data. Check runs indicated that the effect of pilot fuel flow upon efficiency was negligible. Therefore, the pilot was operated at a fuel flow found to give best blow-out limits with the pilot burning alone and the exhaust nozzle unchoked. Fuel was supplied to the two injection manifolds at equal gage pressures.

The data observed covered a range of fuel-air ratios from lean blow-out to about 0.075 and a range of altitudes from 60,500 to 66,500 feet at a flight Mach number of 3.0. For each group of burning data at constant simulated altitude, cold-flow measurements were made. Cold flow signifies no fuel flow to either the pilot nozzle or main manifolds. Cold-flow data, which were used directly in making an air-flow calibration of the engine, also provided information for calculating the combustor efficiency. For all data the engine exhaust nozzle was choked.

Lean blow-outs were detected by means of a continuous recording of the exhaust-nozzle-inlet total pressure. A discontinuous decrease in the pressure to the cold-flow level at station 4 indicated lean blow-out. No rich blow-outs were experienced up to a fuel-air ratio of about 0.075. However, when the fuel distribution in the combustor was poor (because of fouled fuel nozzles), the flow broke down at high engine diffuser recoveries (see Operational Characteristics in RESULTS AND DISCUSSION). The breakdown usually caused combustor blow-out.

The symbols and procedures for calculating the variables considered in this report are shown in appendixes A and B, respectively.

RESULTS AND DISCUSSION

Diffuser Characteristics

The variation of engine-inlet-air flow with free-stream total pressure is shown in figure 5. This figure shows that engine air flow was directly proportional to free-stream total pressure, which indicates that A_0/A_3 did not change appreciably over the range of altitudes which were simulated.

By throttling the exhaust nozzle with the valve in the spray-cooler section, it was determined that for nonburning conditions the critical (maximum) ratio of diffuser-exit total pressure to free-stream total pressure was 0.66. This critical recovery ratio is typical of current diffuser designs. Simulation of subcritical operation of the diffuser was impossible, because the diffuser was inherently unstable at a Mach number of 3.0, and this instability destroyed flow simulation at the engine inlet (see ref. 1).

Mach number profiles at a location in the subsonic portion of the diffuser are shown in figure 6 for a range of fuel-air ratios from zero to 0.0769. These profiles were obtained from data observed at station 2

(12 in. upstream of the plane of the flame holder). The general level of these Mach number profiles reflected the combustor temperature ratio and increased with decreasing fuel-air ratio. The Mach number near the inner body wall was lower for all fuel-air ratios than the Mach number near the outer wall. This effect was probably due to a larger initial boundary layer formed from the supersonic-diffuser cones. Separation of the flow from the inner body wall occurred for cold flow and may have been present for the burning range of fuel-air ratios. However, if separation was present under burning conditions, flow reattachment apparently occurred upstream of station 2.

Combustor Performance

The combustor performance is described by figure 7(a), where the variation of combustor efficiency with fuel-air ratio is shown, and by 7(b), which presents the combustor pressure ratio. Environmental conditions associated with the combustor are shown in figures 7(c) and 7(d), where the variation, respectively, of exhaust-nozzle-inlet total pressure and combustion-chamber-inlet Mach number with fuel-air ratio are shown. The altitude range covered was from 60,500 to 66,500 feet. Lean blow-out, denoted by the solid symbols, effectively limited burning operation to fuel-air ratios richer than about 0.029.

The combustor efficiency (fig. 7(a)) reached a maximum value of about 0.90 at fuel-air ratios between 0.04 and 0.05. At fuel-air ratios leaner than 0.04, the combustor efficiency decreased rapidly with decreasing fuel-air ratio. For operation at fuel-air ratios progressively richer than abut 0.05, the combustor efficiency decreased slowly to a level of about 0.76 at a fuel-air ratio of 0.075. For the range of altitudes and fuel-air ratios investigated, the combustor efficiency was practically unaffected by changes in simulated altitude. As stated previously (see INTRODUCTION), the engine was required to operate at an efficiency of about 0.90 for the fuel-air ratio range from 0.035 to 0.065. The combustor efficiency thus approximated the design requirements except for the small range of fuel-air ratios between 0.035 and about 0.038.

For operation at fuel-air ratios between 0.04 and 0.075 the combustor pressure ratio (fig. 7(b)) was about 0.92. With no combustion, the momentum pressure loss was zero, leaving only the friction losses, which gave a combustor pressure ratio of 0.78. For fuel-air-ratio increases above 0.04, the corresponding increase of momentum pressure loss was almost exactly compensated by a decrease in friction pressure loss caused by the progressively decreasing combustion-chamber-inlet Mach number. For operation at fuel-air ratios below 0.04, the decrease in the momentum pressure loss was more than offset by the increase in the friction pressure loss.

The exhaust-nozzle-inlet total pressure (fig. 7(c)) increased continuously with increasing fuel-air ratio for a given altitude, thus reflecting the increasing exhaust-gas temperature. The range of nozzle-inlet pressures covered in this investigation was from 1240 to 2592 pounds per square foot absolute.

The combustion-chamber-inlet Mach number (fig. 7(d)) decreased from 0.21 at a fuel-air ratio of 0.03 to 0.15 at fuel-air ratios of 0.065 and above. With no combustion in the engine, this Mach number was about 0.31.

Thrust Output

For the free-jet method of investigating ram-jet-engine performance, it was convenient to determine an internal thrust (see appendix B) which included all the forces acting on the engine due to the captured stream tube. Thus the additive drag was already deducted from the internal thrust. At a fuel-air ratio of 0.07 and an altitude of 63,800 feet, the internal thrust coefficient was 0.73 as shown in figure 8. This internal thrust was not optimum for Mach number 3.0 operation, because the diffuser recovery was 0.55 rather than the critical value of 0.66. When the combustor and exhaust-nozzle geometries are assumed to remain fixed, the internal thrust could be optimized for operation at 0.07 fuel-air ratio by redesigning the diffuser inlet so that critical pressure recovery would be obtained. The optimum internal thrust was calculated by assuming zero additive drag for the redesigned fixed-geometry inlet and the combustor-efficiency - fuel-air ratio relations of figure 7(a). The optimum internal thrust coefficient is shown on figure 8, and a value of 1.15 was obtained at a fuel-air ratio of 0.07. Thus an internal thrust increase of 57 percent would be possible by optimization of the diffuser for operation at Mach number 3.0. The internal thrust was also calculated for leaner fuel-air ratios with the same fixed-geometry optimized inlet and flight exhaust nozzle as shown by the dashed curve of figure 8. While this improvement in internal thrust coefficient by redesign of the inlet is theoretically possible for the specific set of flight conditions assumed, it is important to consider that the engine geometry used in this investigation was apparently a compromise to give acceptable performance over the broad range of the engine flight conditions.

The internal thrust presented was determined by using the inlet total momentum (see appendix B). However, the thrust is usually calculated by using free-stream total momentum. The difference in magnitude between these total momentums is equivalent to the additive drag (see ref. 2). The additive drag coefficient was 0.257 for operation at Mach number 3.0. Use of the usual thrust (based on free-stream total momentum) requires that the additive drag be considered as part of the external engine drag. The adoption of an internal thrust using inlet total momentum includes additive drag, and only external pressure and friction drags need be considered in addition to determine the net thrust of the engine.

Operational Characteristics

With respect to operational characteristics, the engine performed smoothly. In a few instances, however, poor fuel distribution due to malfunctioning of the fuel nozzles caused burning to become so rough that the normal shock was expelled from the diffuser, which in turn caused the supersonic flow to break down. On one such occasion, measurement of combustor pressure fluctuations with high-frequency pressure detectors supported this explanation of flow breakdown. These pressure measurements showed that the flow breakdowns were immediately preceded by instantaneous diffuser total-pressure recoveries of about critical level. Maintenance of the variable-area fuel nozzles was a critical item. It was difficult to operate the engine for more than a few hours without several of the variable-area fuel nozzles becoming inoperative. Malfunctioning of these nozzles was due to the presence of dirt and pipe scale in the fuel supplied to the engine. This foreign material in the fuel obstructed many of the small flow channels within the nozzles and caused troublesome sticking of the pintle stems in their guides. In later investigations this fuel nozzle problem was minimized by the installation of additional filters in the fuel lines.

SUMMARY OF RESULTS

The performance of a 20-inch-diameter ram-jet engine was investigated in a free-jet facility at Mach number 3.0 (inlet total temperature, 1100° R) over a range of simulated altitudes from 60,500 to 66,500 feet. The following results were obtained:

1. The maximum combustor efficiency, about 0.90, occurred at fuel-air ratios between 0.04 and 0.05 over the entire range of simulated altitudes. The range of exhaust-nozzle total pressures was from 1240 to 2592 pounds per square foot absolute. Design requirements for a combustor efficiency of about 0.90 were thus nearly fulfilled except for the small range of fuel-air ratios between 0.035 and about 0.038.

2. Lean blow-out was encountered for fuel-air ratios leaner than approximately 0.029.

3. At 63,800 feet altitude and 0.07 fuel-air ratio the diffuser total-pressure recovery was 0.55 and the internal thrust coefficient was 0.73. The critical value of the diffuser total-pressure recovery was 0.66.

4. At a fuel-air ratio of 0.065 and for the range of altitudes investigated, the combustion-chamber-inlet Mach number was 0.15 and the combustor pressure ratio was 0.92.

Lewis Flight Propulsion Laboratory
National Advisory Committee for Aeronautics
Cleveland, Ohio

2724

[redacted]

APPENDIX A

SYMBOLS

The following symbols are used in this report:

A	area, sq ft
B	fraction of supersonic-nozzle jet flow entering engine inlet
C_d	discharge coefficient
C_T	internal thrust coefficient
F_i	internal thrust, lb
F_n	net thrust, lb
f/a	engine fuel-air ratio
(f/a)'	ideal fuel-air ratio
$(f/a)_p$	fuel-air ratio of the preheater
$(f/a)_s$	stoichiometric fuel-air ratio
g	acceleration due to gravity, ft/sec^2
M	Mach number
m	mass flow, slugs/sec
P	total pressure, lb/sq ft abs
p	static pressure, lb/sq ft abs
q	dynamic pressure, lb/sq ft
R	gas constant, ft-lb/(lb)(^oR)
S	total momentum
T	total temperature, ^oR
t	static temperature, ^oR
V	velocity, ft/sec
W	engine inlet-air-flow rate (containing preheater products of combustion), lb/sec

[redacted]

W_a	flow rate of air to preheater, lb/sec
$W_{f,e}$	flow rate of fuel to engine, lb/sec
$W_{f,p}$	flow rate of fuel to preheater, lb/sec
$\int_{A_{ci}} p_x dA$	force parallel to center line of engine due to static pressure acting on inner body cones and across inlet annulus, lb
$\int_{A_{se}} p_x dA$	force parallel to center line of the engine due to static pressure on exterior of engine, lb
$\int_{A_{se+st}} p_x dA$	force parallel to center line of engine due to static pressure acting on exterior surface of engine and on exterior surface of diverging entering stream tube, lb
$\int_{A_{se+st}} \sigma_x dA$	force parallel to center line of engine due to skin friction acting on exterior surface of engine and on exterior surface of diverging entering stream tube, lb
$\int_{A_{st}} p_x dA$	additive drag, lb
γ	ratio of specific heat at constant pressure to specific heat at constant volume
η	combustor efficiency
ρ	density, lb/cu ft

Subscripts:

av	average
c	cold (i.e. engine not burning)
h	hot (i.e. engine burning)
l	local (at a point in annulus)

Station numbers:

0	free stream
1	lip of inlet cowl

2724

[redacted]

2	subsonic diffuser
3	plane of flame holder (combustion-chamber inlet)
4	exhaust-nozzle inlet
5	exhaust-nozzle minimum area
6	exit plane of flight exhaust nozzle

2724

[redacted]

APPENDIX B

CALCULATIONS

Engine-inlet-air flow. - The engine exhaust nozzle served as a convenient metering orifice for determining the rate of flow of air through the engine for nonburning conditions. Because the diffuser was operated supercritically, the inlet-air flow, at a given altitude, was the same for burning and nonburning conditions. The engine-inlet-air flow was calculated from the mass-flow equation

$$W = \rho_{5,c} C_{d,c} A_5 V_{5,c}$$

which was expressed as

$$W = f(P_{5,c}, C_{d,c}, A_5, T_{5,c}, \gamma_c, M_{5,c}, R_c)$$

where $P_{5,c}$ and $T_{5,c}$ were assumed equal to $P_{4,c}$ and T_0, respectively. The exhaust nozzle was choked so that $M_{5,c} = 1$. $C_{d,c}$ was assumed to be 0.985. Leakage was assumed to be negligible so that for the air-flow calibration the exhaust-nozzle air flow was equal to the inlet-air flow.

Subsonic-diffuser Mach number. - The local Mach number at the position of each total-pressure tap at station 2 was computed from static- and total-pressure survey rakes at station 2 and the equation

$$M_{2,l} = \left\{ \left[\left(\frac{P_2}{p_2} \right)^{\frac{\gamma-1}{\gamma}} - 1 \right] \frac{2}{(\gamma - 1)} \right\}^{\frac{1}{2}}$$

Combustion-chamber-inlet Mach number. - The calculation of the combustion-chamber-inlet Mach number was made by first using the mass-flow equation

$$W = \rho A V$$

or

$$M_{2,av} = \frac{W}{p_2 A_2} \sqrt{\frac{Rt_2}{\gamma g}}$$

to compute an average Mach number at station 2 (different from the local Mach number defined previously). Then the combustion-chamber-inlet Mach number M_3 was computed with one-dimensional-flow relations

[redacted]

defining the process of compression from station 2 to station 3 ($A_2/A_3 = 0.76$). It was assumed that the total and static temperatures at station 2 were equivalent and that no change of total temperature or total pressure occurred between stations 2 and 3.

Engine fuel-air ratio. - The engine fuel-air ratio was defined as the ratio of the engine fuel flow to the unburned air passing through the engine inlet. Leaving the preheater was a gas which had a fuel-air ratio of $(f/a)_p = \frac{W_{f,p}}{W_a}$. It was found that the preheater combustion efficiency was 1.0 to a close approximation. The ratio B of the engine-inlet-air flow to the supersonic-nozzle jet flow was constant for all inlet pressures and temperatures. The unburned air entering the engine was then $BW_a\left[1 - \frac{(f/a)_p}{(f/a)_s}\right]$. Note that this is different from W (fig. 5) which includes preheater products of combustion. The engine fuel-air ratio was then

$$\frac{f}{a} = \frac{W_{f,e}}{BW_a\left[1 - \frac{(f/a)_p}{(f/a)_s}\right]}$$

Since it was more convenient to measure the engine-inlet-air flow W than BW_a, use was made of the following relation:

$$W = B(W_a + W_{f,p}) = BW_a\left[1 + (f/a)_p\right]$$

By rearrangement of the terms in this equation, an equivalent expression for BW_a was

$$BW_a = \frac{W}{\left[1 + (f/a)_p\right]}$$

Substitution of this expression in the f/a equation gave

$$\frac{f}{a} = \frac{W_{f,e}}{W}\left[\frac{1 + (f/a)_p}{1 - \frac{(f/a)_p}{(f/a)_s}}\right]$$

Combustor efficiency. - The combustor efficiency was defined as

$$\eta = \frac{(f/a)'}{f/a}$$

[redacted]

2724

where f/a was given in the preceding paragraph, and $(f/a)'$ was the ideal fuel-air ratio which would have produced the same burner pressure P_4 as was measured for the burning conditions under consideration. Thus, the efficiency was related to burner pressures without considering the combustion temperatures which were difficult to measure.

The calculation of $(f/a)'$ was implemented in the following way: Because the diffuser was operating supercritically, the entering air flow, at a given altitude, was the same for the nonburning and burning conditions and could be expressed as

$$W = \rho_{5,c} C_{d,c} A_5 V_{5,c}$$

and

$$W = \frac{\rho_{5,h} C_{d,h} A_5 V_{5,h}}{1 + \frac{W_{f,e}}{W}}$$

for each case, respectively.

By use of the mass-flow equation, the exhaust-nozzle minimum-area total pressure P_5 was determined for the hot and cold conditions:

$$P_{5,h} = \frac{W\left(1 + \frac{W_{f,e}}{W}\right)}{C_{d,h} A_5 M_{5,h}} \sqrt{\frac{R_h T_{5,h}}{\gamma_h g}} \left(1 + \frac{\gamma_h - 1}{2} M_{5,h}^2\right)^{\frac{\gamma_h + 1}{2(\gamma_h - 1)}}$$

$$P_{5,c} = \frac{W}{C_{d,c} A_5 M_{5,c}} \sqrt{\frac{R_c T_{5,c}}{\gamma_c g}} \left(1 + \frac{\gamma_c - 1}{2} M_{5,c}^2\right)^{\frac{\gamma_c + 1}{2(\gamma_c - 1)}}$$

The first equation was divided by the second and the following assumptions were made:

$$P_{5,c} = P_{4,c}$$

$$P_{5,h} = P_{4,h}$$

$$T_{5,c} = T_{4,c} = T_0$$

$$T_{5,h} = T_{4,h}$$

[redacted]

and

$$C_{d,h} = C_{d,c}$$

Noting that $M_{5,c} = M_{5,h} = 1$, the following was obtained:

$$\frac{P_{4,h}}{P_{4,c}} = \left(1 + \frac{W_{f,e}}{W}\right)\sqrt{\frac{\gamma_c R_h T_{4,h}}{\gamma_h R_c T_0}}\,\frac{\left(\frac{\gamma_h + 1}{2}\right)^{\frac{\gamma_h+1}{2(\gamma_h-1)}}}{\left(\frac{\gamma_c + 1}{2}\right)^{\frac{\gamma_c+1}{2(\gamma_c-1)}}}$$

The exhaust-nozzle-inlet total temperature T_4 as a function of ideal fuel-air ratio can be obtained from reference 3 (for temperatures below the dissociation region) and reference 4 (for temperatures in the disssociation region). Thus, the preceding equation provided a means of determining $(f/a)'$ as a function of the easily measured quantity $P_{4,h}/P_{4,c}$. Thus, both factors of the combustor efficiency expression were determined.

Internal thrust coefficient. - Internal thrust F_i included all the forces acting on the engine surfaces wetted by the captured stream tube; thus additive drag, arising from divergence of the entering stream tube, was also part of the internal thrust. In reference 5 net thrust is defined as

$$F_n = m_6V_6 - m_0V_0 + A_6p_6 - A_0p_0 - \int_{A_{se+st}} (p_x + \sigma_x)dA$$

or

$$F_n = m_6V_6 - m_0V_0 + A_6p_6 - A_0p_0 - \int_{A_{se+st}} \sigma_x dA - \int_{A_{se}} p_x dA - \int_{A_{st}} p_x dA$$

Internal thrust is then

$$F_i = F_n + \int_{A_{se+st}} \sigma_x dA + \int_{A_{se}} p_x dA = m_6V_6 + A_6p_6 - m_0V_0 - A_0p_0 - \int_{A_{st}} p_x dA$$

Internal thrust, in coefficient form, is then

$$C_T = \frac{m_6V_6 - m_0V_0 + A_6p_6 - A_0p_0 - \int_{A_{st}} p_x dA}{A_3q_0}$$

[redacted]

From this definition, it is evident that by subtracting the external skin friction and external drag coefficients from the internal thrust coefficient that the net thrust coefficient results. Evaluation of the various terms in the expression for F_i was accomplished as follows: The term m_6V_6 was evaluated by use of reference 6, where actual thrust measurements were made for a nozzle having an expansion ratio A_6/A_5 of 1.69 as in the flight engine. Because a greater T_4/T_0 can be obtained with inlet air the oxygen content of which has not been depleted, the exhaust-nozzle inlet total pressure must be corrected before the data of reference 6 can be applied. Therefore, new P_4 values were calculated (with the mass-flow equation at the choked exhaust nozzle) by assuming that the combustor-efficiency - fuel-air-ratio relations shown in figure 7(a) were applicable to the flight combustor. The calculated values of P_4 were slightly higher than measured values of P_4, because the available oxygen in the flight engine inlet air would be slightly greater.

The terms m_0V_0, A_6p_6, and A_0p_0 were functions of P_0 only.

The term $\int_{A_{st}} p_x dA$ or $S_1 - S_0$, is commonly referred to as additive drag. Reference 2 defines additive drag as the increment of axial pressure force (greater than free-stream static force) acting upon the diverging portion of the stream tube entering the engine. Symbolically, additive drag may be defined as

$$S_1 - S_0 = \int_{A_{st}} p_x dA = \left(m_0V_1 + \int_{A_{ci}} p_x dA\right) - (p_0A_0 + m_0V_0)$$

By the use of inlet instrumentation at station 1 and on the diffuser cones it was possible to evaluate the preceding terms.

REFERENCES

1. Wentworth, Carl B., Hurrell, Herbert G., and Nakanishi, Shigeo: Evaluation of Operating Characteristics of a Supersonic Free-Jet Facility for Full-Scale Ram-Jet Investigations. NACA RM E52I08, 1952.

2. Sibulkin, Merwin: Theoretical and Experimental Investigation of Additive Drag. NACA RM E51B13, 1951.

3. Turner, Richard L., and Bogart, Donald: Constant-Pressure Combustion Charts Including Effects of Diluent Addition. NACA Rep. 937, 1949. (Supersedes NACA TN's 1086 and 1655.)

[redacted]

4. Mulready, Richard C.: The Ideal Temperature Rise Due to the Constant Pressure Combustion of Hydrocarbon Fuels. M.I.T. Meteor Rep. UAC-9, Res. Dept., United Aircraft Corp., July 1947. (BuOrd Contract NOrd 9845.)

5. Dailey, C. L., and Wood, F. C.: Ram Jet Performance Methods. Rep. 4-1, Aero. Lab., Univ. Southern Cal., June 13, 1947. (Navy Contract NOa(s) 8257.)

6. Krull, H. George, and Steffen, Fred W.: Performance Characteristics of One Convergent and Three Convergent-Divergent Nozzles. NACA RM E52H12, 1952.

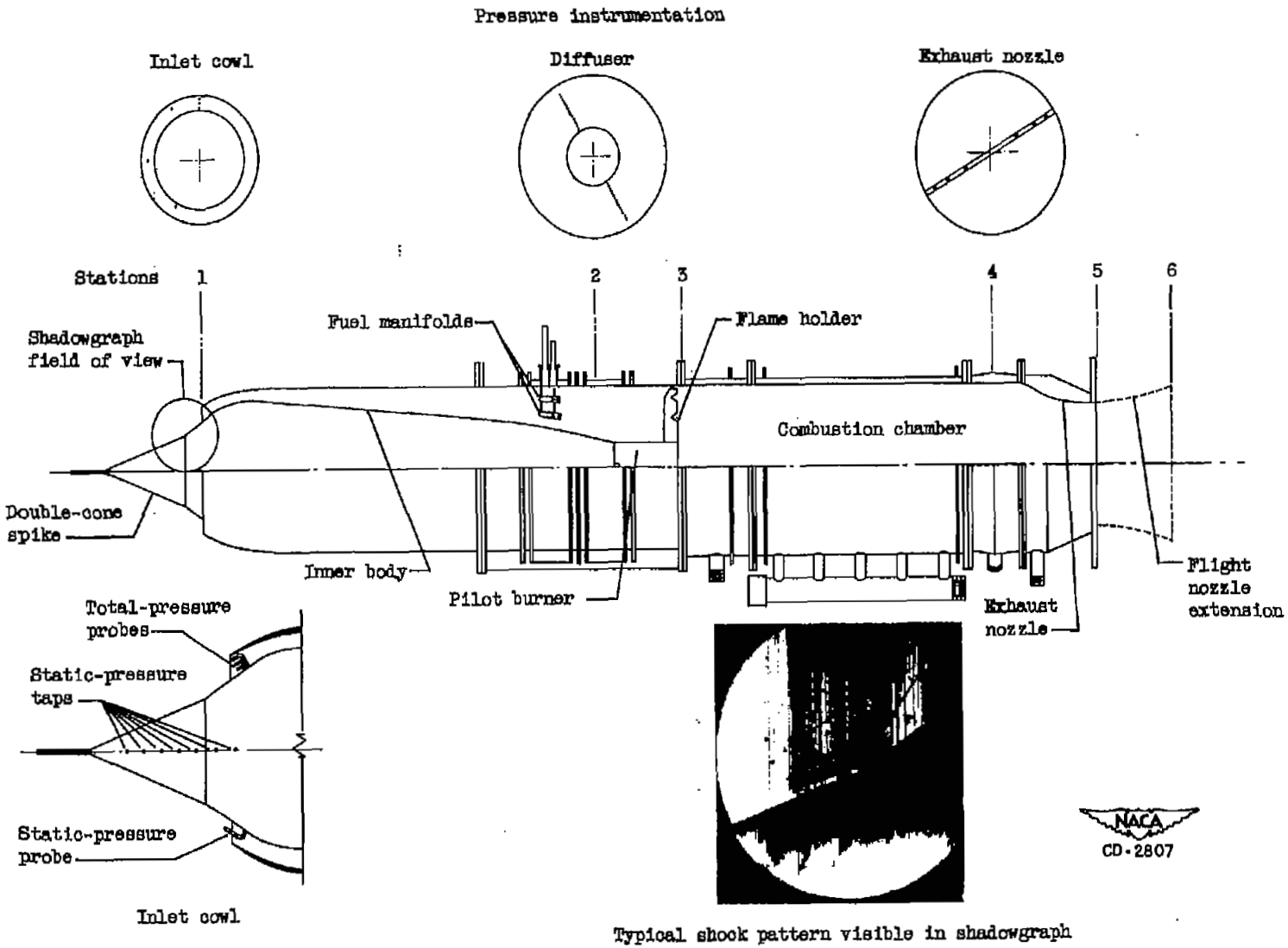

Typical shock pattern visible in shadowgraph

Figure 1. - Stations, instrumentation, and typical shock pattern of 20-inch ram-jet engine. Station 0 is in surge tank ahead of supersonic nozzle.

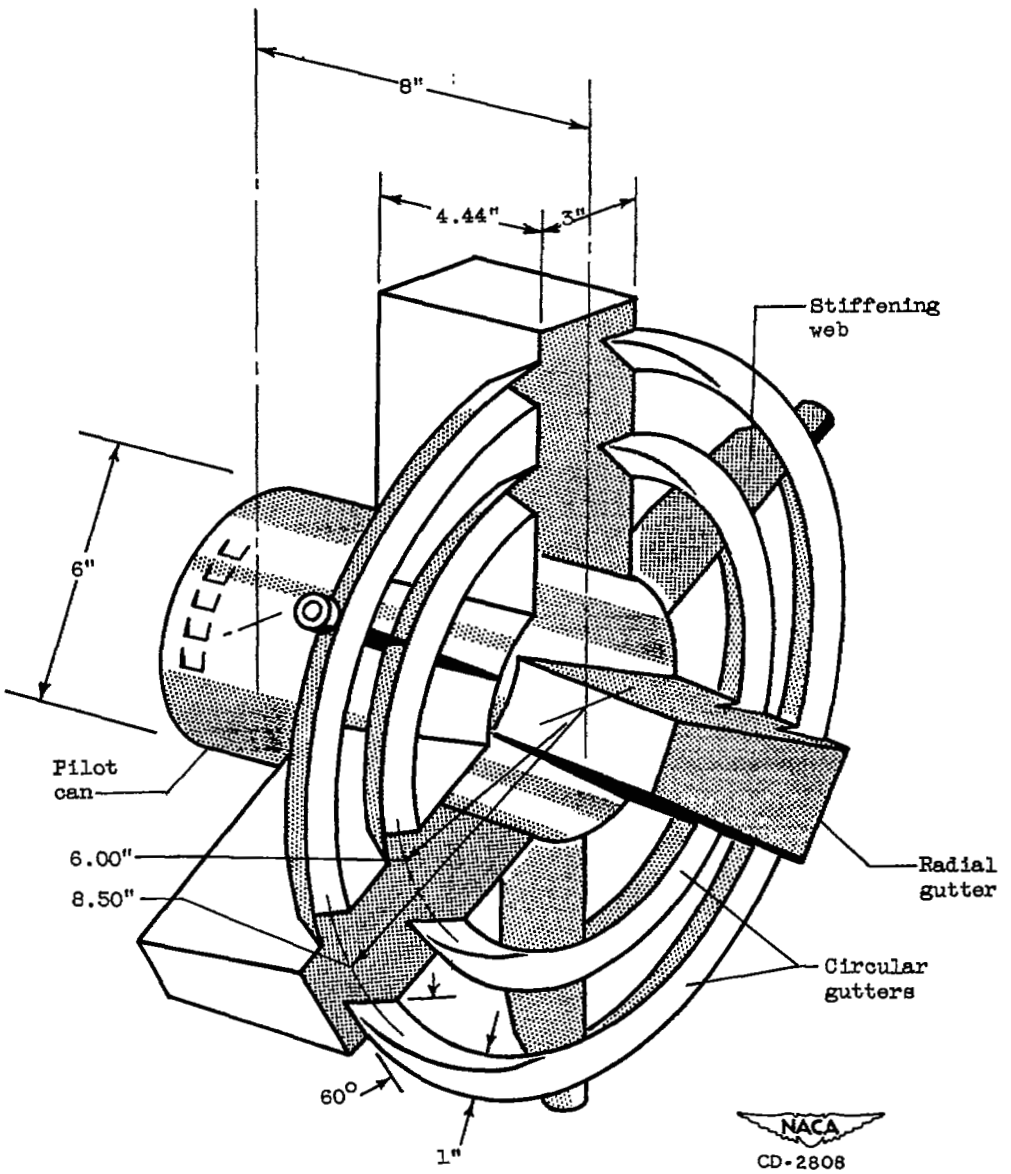

Figure 2. - Diagram of flame holder.

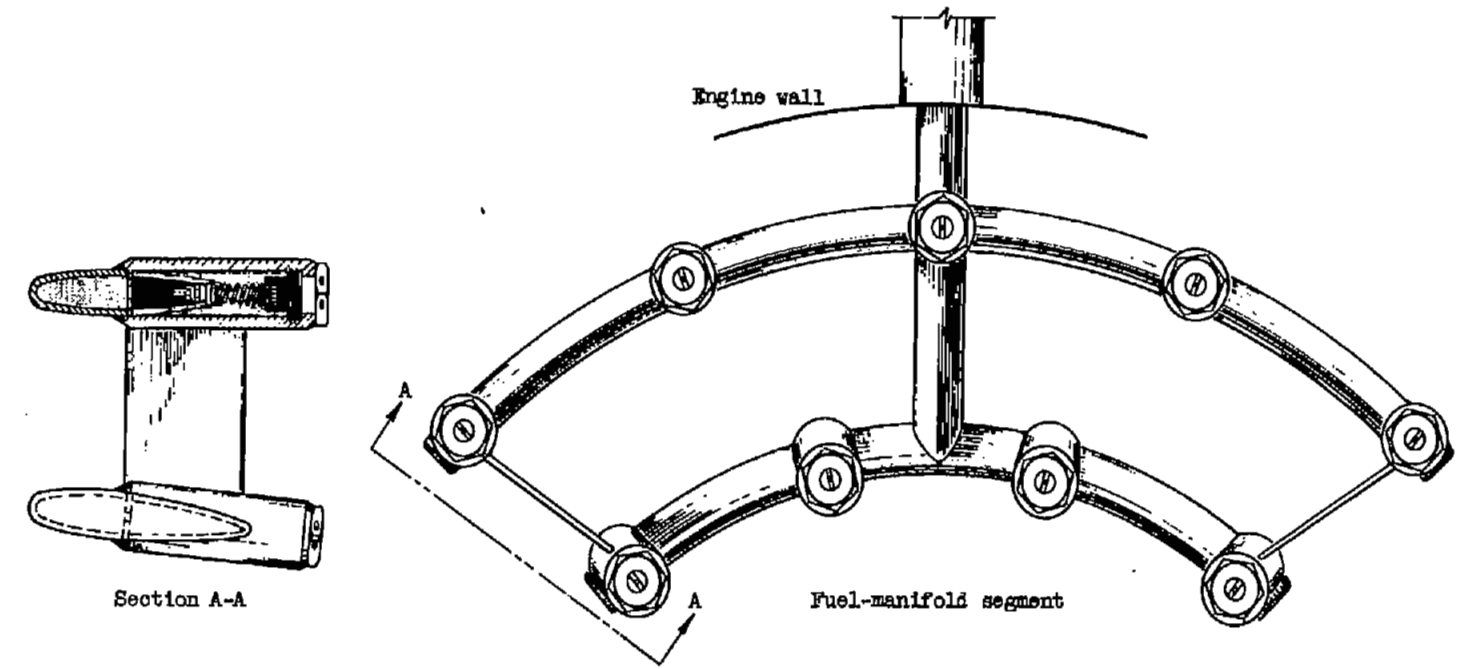

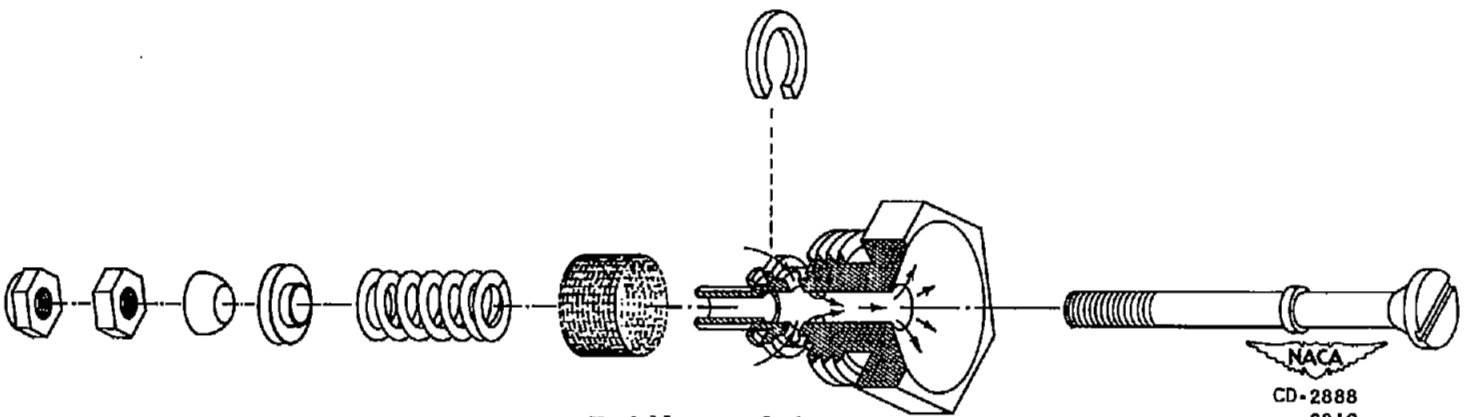

Variable-area fuel nozzle

Figure 3. - Fuel system.

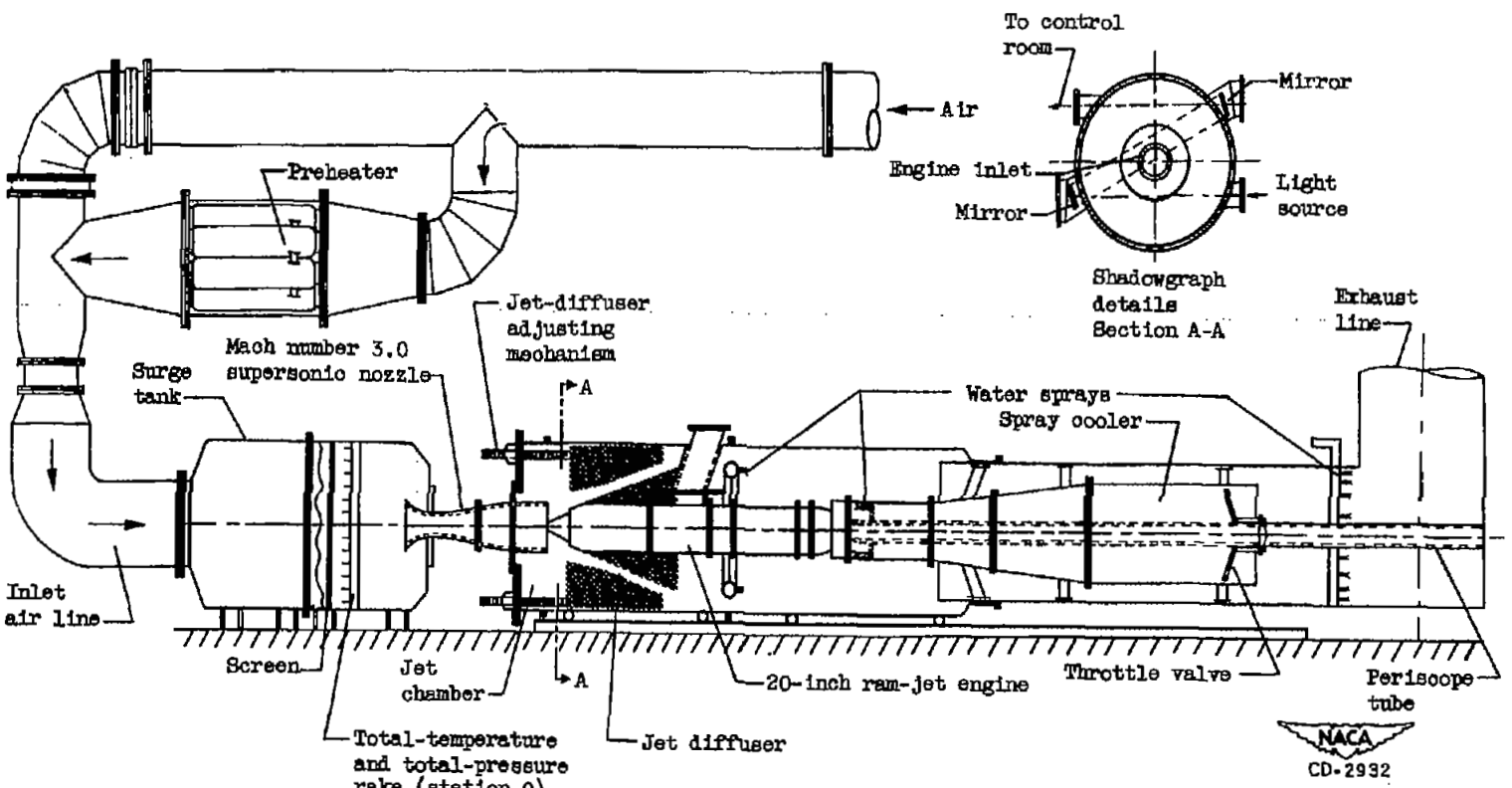

Figure 4. - Schematic diagram of 20-inch ram-jet engine installed in a free-jet facility at Mach number 3.0.

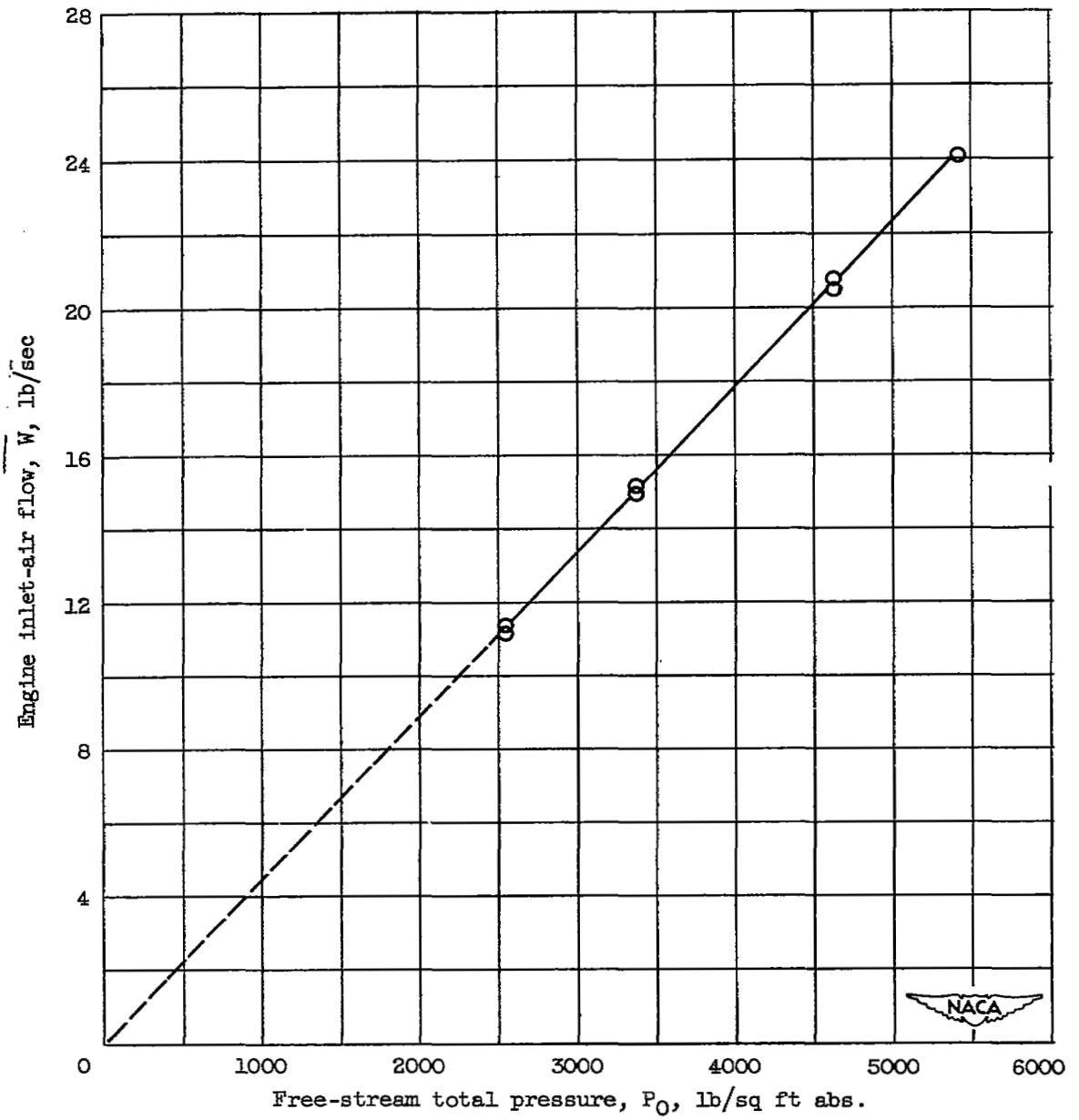

Figure 5. - Engine inlet-air flow as function of free-stream total pressure for supercritical operation. Free-stream total temperature, 1100° R.

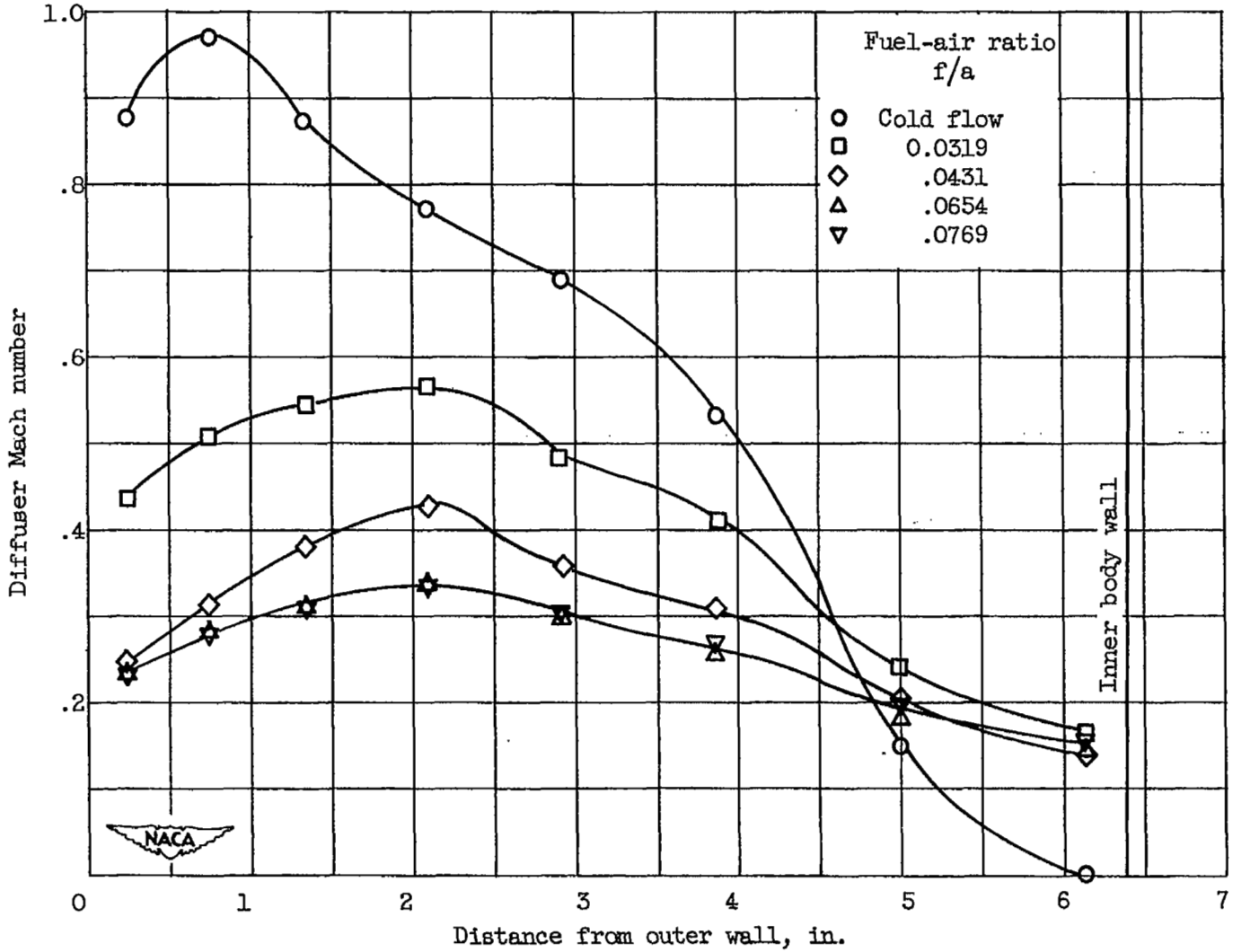

Figure 6. - Comparison of diffuser Mach number profiles at various fuel-air ratios. Measuring station 12 inches upstream of plane of flame holder.

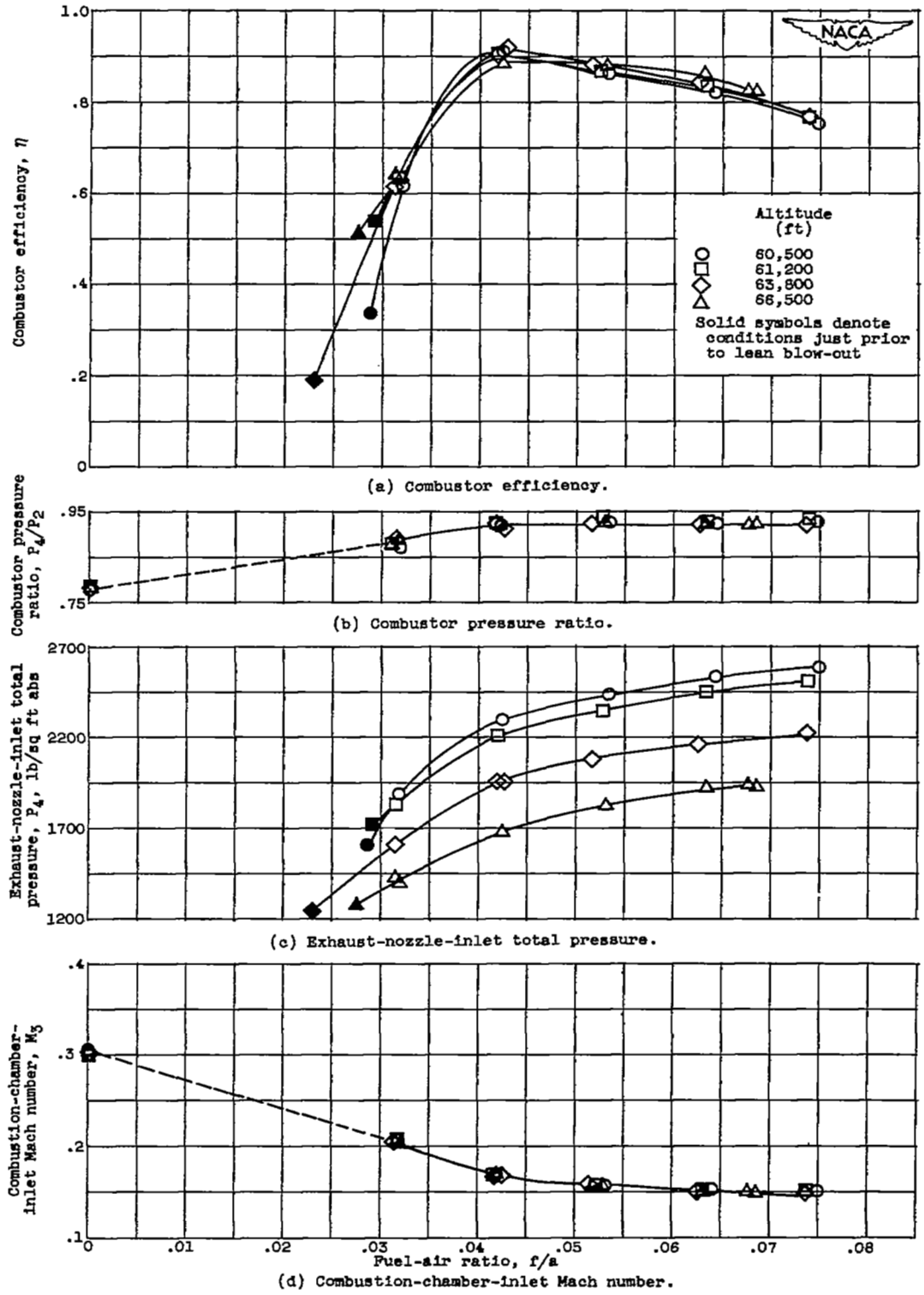

Figure 7. - Altitude effect of fuel-air ratio on engine performance.

[redacted]

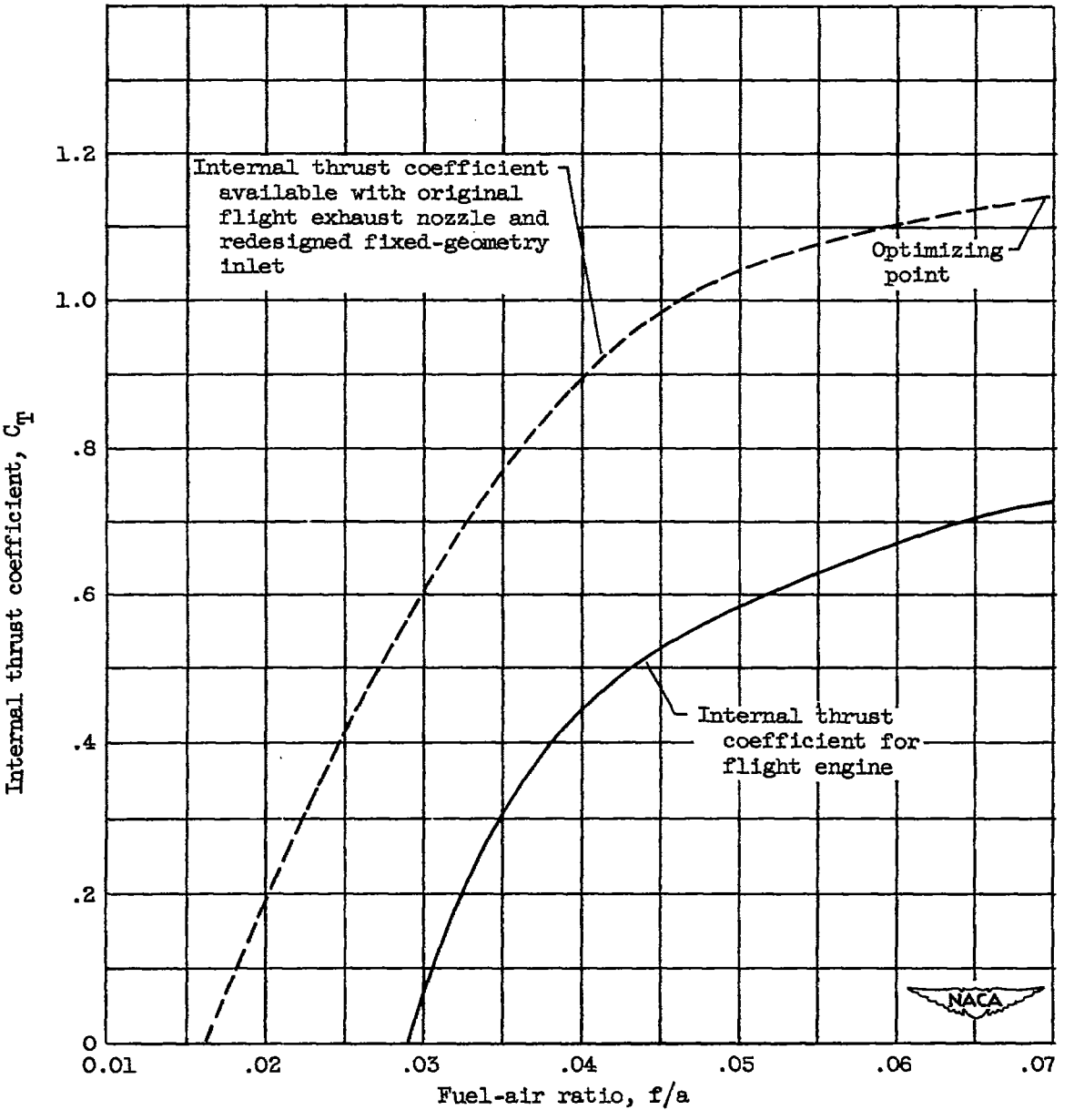

Figure 8. - Variation of internal thrust coefficient with fuel-air ratio. Simulated altitude, 63,800 feet.

NACA-Langley - 6-15-53 - 500